Available online at www.sciencedirect.com
SCIENCE DIRECT®
Journal of Magnetic Resonance 168 (2004) 246–251
JMR Journal of Magnetic Resonance
www.elsevier.com/locate/jmr

Magnetic material arrangement in oriented termites: a magnetic resonance study

O.C. Alves,[a,*] E. Wajnberg,[b] J.F. de Oliveira,[b] and D.M.S. Esquivel[b]

[a] *Dept de Físico-Química, Universidade Federal Fluminense, Niterói, Rio de Janeiro, 14020-150, Brazil*
[b] *Centro Brasileiro de Pesquisas Físicas, Rio de Janeiro, 22290-180, Brazil*

Received 18 December 2003; revised 9 March 2004
Available online 2 April 2004

Abstract

Temperature dependence of the magnetic resonance is used to study the magnetic material in oriented *Neocapritermes opacus* (N.o.) termite, the only prey of the migratory ant *Pachycondyla marginata* (P.m.). A broad line in the $g = 2$ region, associated to isolated nanoparticles shows that at least 97% of the magnetic material is in the termite's body (abdomen + thorax). From the temperature dependence of the resonant field and from the spectral linewidths, we estimate the existence of magnetic nanoparticles 18.5 ± 0.3 nm in diameter and an effective magnetic anisotropy constant, K_{eff} between 2.1 and 3.2×10^4 erg/cm^3. A sudden change in the double integrated spectra at about 100 K for N.o. with the long body axis oriented perpendicular to the magnetic field can be attributed to the Verwey transition, and suggests an organized film-like particle system.

Keywords: Magnetic material; Orientation; Termite; Magnetic resonance

1. Introduction

The *Pachycondyla marginata* (P.m.) ant presents a migratory behavior, relocating the nest sites at irregular time intervals [1]. Most of the migratory process takes place in darkness during the dry/cold season. The migration is significantly oriented at an angle of 13° relative to the magnetic North–South axis [2]. Animal orientation relies on multiple cues, which may sometimes interact in complex ways, but the only possible cue to yield this migratory information is the geomagnetic field [3]. This magnetic orientation hypothesis gains in plausibility considering that magnetic iron oxides have been found in this ant [4]. Isolated magnetic nanoparticles and aggregates were inferred in the abdomen by magnetic resonance [5] and supported by induced remanent magnetization temperature dependence measurements [6].

The P.m. ant is an obligate termite predator that conducts well-organized predatory raids toward the nests of its only prey, the *Neocapritermes opacus* (N.o.) termite. Target termite nests are up to 38 m from the ant colony, and raids on these nests occur both by day and night, and can last for more than 24 h [1]. The chemical transformation of food and nest building by termites have an important role in nutrition cycles and structural change of soil in forest and others vegetable ecosystems [7]. N.o. is usually found in active or inactive nests of other species, it lives on vegetables and wood garbage and is considered one of the most dangerous sugarcane pests.

Due to the termite's ecological aspects, particularly the prey–predator relation, it became a very attractive species for magnetic materials studies in social insects. Magnetic resonance (MR) has proved to be a useful technique for these studies because of the resonance spectra dependence on the magnetic structure size and shape. This technique encompasses enough sensitivity to study inorganic precursors [8], as well as magnetic materials in ants and bees [5,9,10]. In this paper, we report on the temperature dependence of the MR spectra of

* Corresponding author. Fax: +55-21-21417540.
E-mail addresses: cambraia@cbpf.br (O.C. Alves), elianew@cbpf.br, darci@cbpf.br (E. Wajnberg).

1090-7807/$ - see front matter © 2004 Elsevier Inc. All rights reserved.
doi:10.1016/j.jmr.2004.03.010

N.o. termites sections, head and body (thorax + abdomen), to investigate the presence and to compare the properties of the magnetic particles present in these sections.

2. Experimental

N.o. termites were collected in Campinas, São Paulo, in the Southeast of Brazil, found inside the P.m. nests. Termites were extensively washed with 80% (v/v) ethanol and conserved in this solution. Samples were transferred to MR quartz tubes and sealed under nitrogen flux to prevent oxygen contributions to the MR signals at low temperatures (below 80 K).

Samples consist of three heads and one oriented body (abdomen + thorax) of worker termites cooled in a 3.4 kOe magnetic field. The orientation effects were studied with the body fixed in MR tubes with vacuum grease, with the magnetic field parallel (z direction), N.o.$_{\parallel}$, and perpendicular (y direction), N.o.$_{\perp}$ to long body axis, as shown in Fig. 1. Heads were not oriented. Four individual bodies were used for repeated temperature variation experiments. The results are the average values obtained with three and two experiments for N.o.$_{\perp}$ and N.o.$_{\parallel}$, respectively.

Measurements were performed with a commercial X-band ($\upsilon = 9.442476$ GHz) MR spectrometer (Bruker ESP 300E) operating at a microwave power of 4 mW with a 100 kHz modulation frequency and a modulation field of about 2 Oe in amplitude. A helium flux cryostat (Air products LTD-3-110) was used to control the temperature with an Au–Fe × chromel thermocouple just below the samples.

The absorption derivative resonant field, H_R, and the peak-to-peak linewidth, ΔH, were obtained with the WINEPR software (Bruker), taking H_R at the maximum of the absorption spectra (first integral). Fittings were performed with Origin (Microcal) software.

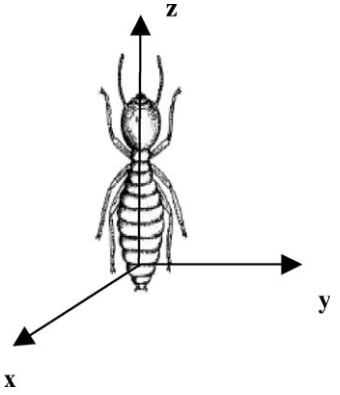

Fig. 1. Termite axis scheme. N.o.$_{\parallel}$, magnetic field parallel to z-axis (the N.o. body long axis), N.o.$_{\perp}$, magnetic field parallel to y-axis direction.

3. Results

Fig. 2 shows the N.o.$_{\perp}$ and single head derivative MR spectra at different temperatures. At temperatures higher than 15 ± 4 K both head and N.o.$_{\perp}$ and N.o.$_{\parallel}$ (not shown) body spectra consist of a broad ($\Delta H > 1100$ Oe) line at $g \approx 2.0$. The signal intensity decreases and the linewidth increases as temperature decreases.

At temperatures below 20 K (not shown) the broad line in the head spectra disappears and two narrow lines at $g = 2.066$ and $g = 4.3$ are easily observed (arrows on Fig. 2). Their signal intensity decreases strongly with increasing temperatures and it is not observed at high temperatures. The temperature dependences of N.o.$_{\parallel}$ or N.o.$_{\perp}$ spectra are similar. The spectra broaden asymmetrically and shift to lower magnetic fields when temperature decreases. This is the typical high temperature behavior found for different superparamagnetic nanoparticles immersed in an inert matrix [11], in glycerol [12], in solid kerosene [13], in sol-gel glass [14,15] and also observed for the MR high field component of P.m. ant abdomen spectra [5].

Fig. 3 shows the N.o.$_{\parallel}$, N.o.$_{\perp}$, and N.o head resonance linewidth temperature dependences. The experimental data were fitted with the expression (1) for the entire temperature range of the observation

$$H = \Delta H^0 \tan h(\Delta E/2kT), \tag{1}$$

where $\Delta H^0 = 5g\beta Sn/d^3$ and $\Delta E = KV$ is mainly associated to the magnetic energy barrier height, K is the magnetic anisotropy constant and V is the particle volume. The ΔH^0 prefactor, which is the ΔH low temperature limit, includes the Bohr magneton, β, the spin associated to the magnetic nanoparticle center, S, the number of magnetic centers in the particle, n, and the

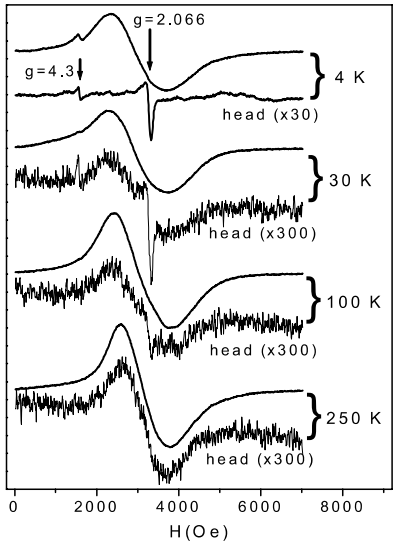

Fig. 2. Temperature dependence of N.o.$_{\perp}$ and a single head magnetic resonance spectra.

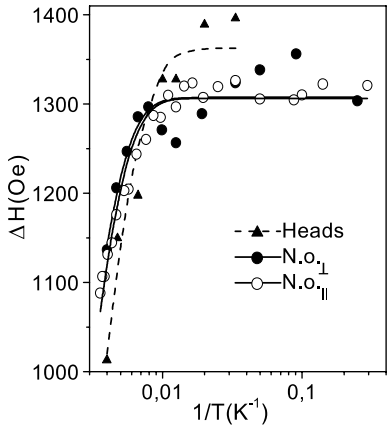

Fig. 3. Spectra linewidth temperature dependence. The solid and dashed lines are the best fits of Eq. (1) for the body (N.o.$_{\parallel}$ and N.o.$_{\perp}$) and head data, respectively, with the parameters given in Table 1.

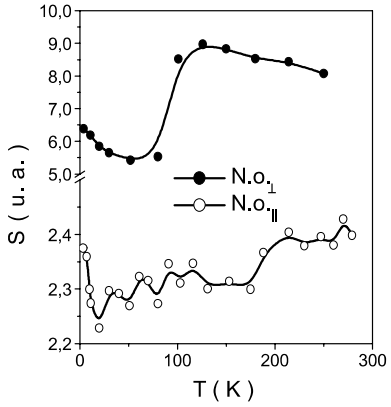

Fig. 5. Temperature dependence of MR spectra absorption area, $S = I_{pp}\Delta H^2$, showing that at 250 K the N.o.$_{\perp}$ value is almost three times that of N.o.$_{\parallel}$.

particle–particle distance, d. The best-fit parameters are listed in Table 1 and, for comparison, the P.m. abdomen values are also given.

Fig. 3 and the data in Table 1 show that the N.o.$_{\parallel}$ and N.o.$_{\perp}$ linewidth data present, within the experimental error, the same behavior with $KV = (9.1 \pm 0.5) \times 10^{-21}$ J, while for N.o. head $KV = (6.7 \pm 0.4) \times 10^{-21}$ J. The same is observed for the limiting low temperature value (the prefactor ΔH^0) which is distinguishable only for the head part.

Table 1
N.o. termite and P.m. migratory ant fitting parameters of Eq. (1)

	H_R^0 (Oe)	$\Delta E/2k$ (K^{-1})	Temperature fitting range
N.o.$_{\parallel}$	1306 ± 4	320 ± 4	4–279 K
N.o.$_{\perp}$	1307 ± 10	336 ± 20	4–279 K
N.o. head	1363 ± 19	242 ± 13	>20 K
P.m. abdomens[a]	1373 ± 10	272 ± 7	>70 K

[a] From [5].

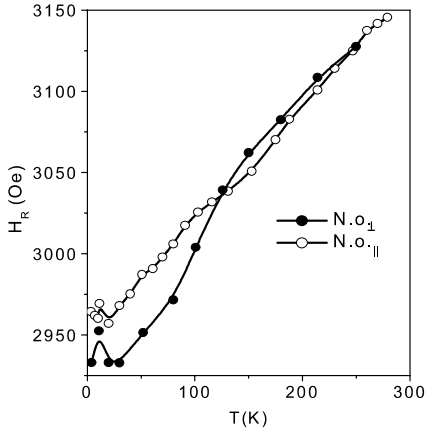

Fig. 4. Temperature dependence of resonant field, H_R. Solid lines are guide to the eyes.

The N.o.$_{\parallel}$ and N.o.$_{\perp}$ resonant magnetic field (H_R) temperature dependences are similar (Fig. 4). A smooth inflection is more easily observed in the 100 K region for the perpendicular orientation. The head data also present a shift in this temperature range, but it is within the error bars much larger than those of the body data, because of the $g = 2.066$ superimposed line (not shown).

The peak-to-peak amplitude, I_{pp} (not shown) and the double integration of the MR (area under absorption curve) S are proportional to the magnetic particle number. At 250 K the second integration of the N.o.$_{\perp}$ body line is 250 times larger than that of a single head while this value decreases to 70 for the N.o.$_{\parallel}$ line. The magnetic material is predominantly in the N.o. body (about 99 and 97% considering the N.o.$_{\perp}$ and N.o.$_{\parallel}$ body orientation, respectively). The N.o.$_{\perp}$ area values are almost three times those of the N.o.$_{\parallel}$, showing a lower number of magnetic particles in the specimens used for the parallel orientation (Fig. 5). Variability of the amount of magnetic material in insects has already been observed in bees and termites [16,17].

The S temperature dependence is sensitive to the N.o. body orientation relative to the magnetic field. The N.o.$_{\perp}$ presents a sudden increase at nearly 90 ± 10 K, not observed for N.o.$_{\parallel}$, strengthening the behavior observed for the ΔH (Fig. 3) and H_R (Fig. 4) temperature dependences.

4. Discussion

At low temperatures the MR spectra of heads presents only two lines at $g = 4.3$ and $g = 2.066$. The first one was observed in other social insects [5,9,10] and was associated to magnetically isolated high spin ($S = 5/2$) Fe^{3+} ions in a low symmetry environment [18]. Its signal intensity decreases strongly with increasing temperatures and it is not observed at high temperatures. A line

similar to the $g = 2.066$ one was observed in horse spleen ferritin solution [19] and when ferritin core is developed from Fe^{2+} and O_2 in apoferritin. It was suggested that it involves a hydroxyl radical formation as a by-product of the core formation, once that iron under aerobic conditions is capable of producing these radicals [20]. It was neither observed in the N.o. body nor in P.m. and honeybee abdomens, either because of the much higher intensity of the broad line in these samples or because it is not formed.

The broad line could not be followed to temperatures lower than 20 K, suggested as the Neel temperature of uncompensated spins in horse spleen ferritin [19]. Ferritin was found in the endoplasmatic reticulum and secretory pathway of nine families from six insect orders [21]. Electron microscopy analysis suggest that microcrystals containing iron found in leafhoppers gut are comprised of ferritin with 6 nm core diameters [22], similar to those reported for mammalian ferritin.

Considering the system as composed by spherical nanoparticles, with no demagnetization field contribution, the resonant field is given by $H_R(T) = \omega_R/\gamma - H_A(T)$, where ω_R is the resonance frequency, γ is the gyromagnetic ratio and H_A the effective anisotropy field. Using the experimental values of ω_R and $\gamma = 1.87\times10^7\,\mathrm{Oe^{-1}\,s^{-1}}$ ($g = 2.13$) extrapolated at the high temperature limit ($H_R = 3166$ Oe) at which the H_A is expected to be null, the temperature dependence of H_A is obtained (Fig. 6). For spherical nanoparticles H_A is given by $2K_{eff}/M_S$, where K_{eff} is the effective magnetocrystalline anisotropy density and M_S is the saturation magnetization, characteristic of the magnetic material.

Under the hypothesis of ferritin particles, taking the horse spleen ferritin magnetic moment as $345\mu_B$ [23] and $200\mu_B$ [24], M_S ferritin values are estimated as 16.4 and 28.3 Oe, respectively. From H_A values averaged in the experiment temperature range (Fig. 6), $K = 7.3\times10^2$ and $12\times10^2\,\mathrm{erg/cm^3}$ are calculated, which together with ΔE values from Table 1 yield a diameter larger than 47 nm, which falls outside the insect ferritin ranges. Although the ferritin contribution cannot be completely discarded, the MR spectra may indicate that it is a magnetite core formation in ferritin, as observed in human brain tissues [25] or a ferritin–magnetite transformation. The highly toxic Fe^{2+} is taken by the protein and oxidized, to be stored as less toxic Fe^{3+}, in the form of ferrihydrite [26]. If the ferritin core becomes overloaded or there is a breakdown in the protein's function, a mechanism for Fe^{2+} oxidation is lost, leading to the formation of biogenic magnetite that contains alternating lattice of Fe^{2+} and Fe^{3+} [27].

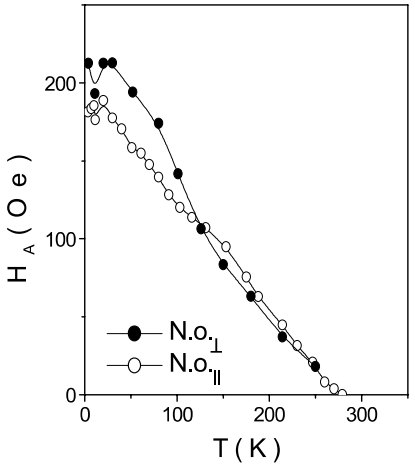

Fig. 6. Temperature dependence of anisotropy field, H_A, calculated from the resonant field curves in Fig. 4.

On the other hand, magnetite is the most common biomineralized material, with $g = 2.12$ [28,29] in good agreement with the limit value calculated above, and M_S as 470 Oe. From the H_A values, K_{eff} values are then obtained as $(2.6\pm0.1)\times10^4$, $(3.2\pm0.2)\times10^4$, and $(2.1\pm0.1)\times10^4\,\mathrm{erg/cm^3}$ for N.o.$_\parallel$, N.o.$_\perp$, and N.o. head, respectively. Using these values and the $\Delta E = KV$ values given in Table 1, the same average magnetic volumes of $(3.2\pm0.3)\times10^3\,\mathrm{nm^3}$ are obtained for body and head particles, and correspond to a diameter of 18.5 ± 0.3 nm. As n is proportional to the particle volume, the prefactors in Table 1 indicate shorter particle–particle distances in the head than in the body.

At low temperatures bulk magnetite undergoes a phase transition already observed by anomalies in electrical and magnetic properties, such as an abrupt changes in K [28] or in the magnetic susceptibility [30]. The intensity and temperature of this transition depend on the stoichiometry [29], impurities or derivative substitutes [31,32] and molar ratio of Fe^{3+} and Fe^{2+} [33]. Nevertheless magnetic properties behavior of layers can differ considerably from bulk behavior as a result of substrate induced strain or relatively large contribution of an altered anisotropy at the interface, associated to different growth technique and/or substrate material [34–36].

A sharp transition was observed in the temperature dependence of the perpendicular resonant field of ultrathin Fe_3O_4 layers grown on different substrate films [34,36]. Its intensity and shape was shown to depend on the thickness of magnetic film. It takes place at about 105 K, for magnetic layer thickness from 5 to 200 nm [36] and is hardly detectable for thickness below 5 nm [34]. This transition was associated to the magnetite Verwey temperature.

The area under the absorption curve, S, was shown to correlate to the magnetic susceptibility in ferrihydrite nanoparticles [37]. The S transition observed is associated to the susceptibility bulk transition cited above, with a modified shape as in a layer structure and the temperature dependence of ΔH and H_R for N.o.$_\perp$

suggest the film-like configuration perpendicular to the resonant field.

5. Conclusions

This paper presents a novel application of MR to determine the organization and magnetic parameters of iron oxide particles in termites. MR data show that 97–99% of the magnetic material is in the N.o. termite body. Magnetization measurements indicate a less asymmetric distribution in another termite species, *Nasutitermes exitious*, with about 77% of the material in the body [17], while 34% of the saturation magnetization comes from the P.m. ant body contribution [41].

The nanoparticles in the head could only be derived from biomineralization and/or cuticular contamination processes [4] while in the body they could be due to biomineralization and the accumulation of ingested materials in the digestive apparatus. Although the latter case cannot be related to a magnetic orientation process, the magnetic anisotropy changes observed and the suggested geometric arrangement indicate that some of the nanoparticles in N.o. body are involved with the magnetoreception process. Although there is no report on magnetoreception for N.o., it was observed in foraging of another termite species, *Trinervitermes geminatus* [38].

Since MR spectra of N.o. oriented parallel ($N.o._{\parallel}$) or perpendicular ($N.o._{\perp}$) to the magnetic field ought to be due to the same particle system, the differences between the parallel and perpendicular orientation behaviors can be related to the magnetic particles arrangement. A particle system in the zx body plane with the easy magnetization axis close to the y direction, perpendicular to the N.o. body axis (Fig. 1) could account for this result. Similarly, magnetite nanoparticles aligned transversely to the body axis on the horizontal plane were observed in the honeybee [16]. This effect was not observed in MR studies of honeybee abdomens [9] because crushing of the sample disrupted the particles arrangement. The present study with an intact oriented sample allowed us to verify the structural organization of the particles in the body of the termite.

A much larger quantity of isolated nanoparticles was found in N.o. termite specie as compared to its predator, the P.m. ant, with similar remanent to saturation magnetization ratio, J_R/J_S, within the magnetite pseudo single domain (PSD) or multi domain (MD) region [42]. These P.m. ant abdomens MR spectra at high temperatures were characterized by two broad main components: the high field ($g \sim 2$) related to isolated magnetic nanoparticles and the low field (g in the range from 5 to 6.3) related to aggregate or large particles [5]. Clusters or larger particles are not observed in N.o. termites, as the low field line is not present in their spectra.

The different magnetic diameters estimated for isolated particles, 18.5 ± 0.3 nm for termites and 13 ± 0.4 nm for ants [5], as well as reported different H_C values (in press, JMMM) suggest that the ant predator does not make direct use of the termite prey magnetic material, no matter whether ingested or biomineralized. Nanoparticle magnetic properties are sensitive to the size, shape, organization, and particle–particle distance. If these particle systems are related to the sensorial system these differences could account for their specific magnetoreception mechanism. While in microorganisms the size and appearance of magnetite biomineralized crystals are specie-specific and uniform within a single cell with a narrow size distribution [39,40], in animals this kind of study is just beginning. In the this context, the differences observed in MR spectra of N.o. termites and P.m. ants, related to the differences in biomineralization and accumulation process of magnetite, should be associated to their role in the predator–prey relationship. This subject opens a branch of study for the biomineralization process under the ecological and evolutionary point of view.

Acknowledgments

We thank Dr. P.S. Oliveira for termite supply, Dr. G. Bemski for the comments and Dr. D. Ellis for carefully reading the manuscript. E.W. and D.M.S.E. thank CNPq and FAPERJ for financial support and J.F.O. thanks the CNPq for a fellowship.

References

[1] I. Leal, P.S. Oliveira, Behavioral ecology of the neotropical termite-hunting ant *Pachycondyla* (= *Termitopone*) *marginata*: colony founding, group-raiding and migratory patterns, Behav. Ecol. Sociobiol. 37 (1995) 373–383.
[2] D. Acosta-Avalos, D.M.S. Esquivel, E. Wajnberg, H.G.P. Lins de Barros, P.S. Oliveira, I. Leal, Seasonal patterns in the orientation system of the migratory ant *Pachycondyla marginata*, Naturwissenchaften 88 (2001) 343–346.
[3] R. Wiltschko, W. Wiltschko, Magnetic Orientation in Animals, Springer, Berlin, 1995.
[4] D. Acosta-Avalos, E. Wajnberg, P.S. Oliveira, I. Leal, M. Farina, D.M.S. Esquivel, Isolation of magnetic nanoparticles from *Pachycondyla marginata* ants, J. Exp. Biol. 202 (1999) 2687–2692.
[5] E. Wajnberg, D. Acosta-Avalos, L.J. El-Jaick, L. Abraçado, J.L. Coelho, A.F. Bakuzis, P.C. Morais, D.M.S. Esquivel, EPR study of migratory ant *Pachycondyla marginata* abdomens, Biophys. J. 78 (2000) 1018–1023.
[6] E. Wajnberg, G. Cernicchiaro, D. Acosta-Avalos, L.J. El-Jaick, D.M.S. Esquivel, Induced remanent magnetization of social insects, J. Magn. Magn. Mater. 2040 (2001) 226–230.
[7] E.R. Laffont, Available from <http://www.unne.edu.ar/cyt/2001/6-Biologicas/B-044.pdf>.
[8] R. Berger, J. Kliava, J.C. Bissey, V. Baietto, Superparamagnetic resonance of annealed iron-containing borate glass, J. Phys. Condens. Matter 10 (1998) 8559–8572.

[9] L.J. El-Jaick, D. Acosta-Avalos, D.M.S. Esquivel, E. Wajnberg, M.P. Linhares, EPR study of Honeybees *Apis mellifera* abdomens, Eur. Biophys. J. 29 (2001) 579–586.
[10] D.M.S. Esquivel, D. Acosta-Avalos, L.J. El-Jaick, A.D.M. Cunha, M.G. Malheiros, E. Wajnberg, M.P. Linhares, Evidence for magnetic material in the fire ant *Solenopsis* sp by electron paramagnetic resonance measurements, Naturwissenschaften 86 (1999) 30–32.
[11] P.C. Morais, M.C.F. Lara, K. Skeff Neto, Electron spin resonance in superparamagnetic particles dispersed in a non-magnetic matrix, Philos. Mag. Lett. 55 (1987) 181–183.
[12] F. Gazeau, V. Shilov, J.C. Bacri, E. Dubois, F. Gendron, R. Perzynski, Y.L. Raikher, V.I. Stepanov, Magnetic resonance of nanoparticles in a ferrofluid: evidence of thermofluctuational effects, J. Magn. Magn. Mater. 202 (1999) 535–546.
[13] K. Nagata, A. Ishihara, ESR of ultrafine magnetic particles, J. Magn. Magn. Mater. 104 (1992) 1571–1573.
[14] R. Berger, J.C. Bissey, J. Kliava, H. Daubric, C. Estournes, Temperature dependence of superparamagnetic resonance of iron oxide nanoparticles, J. Magn. Magn. Mater. 234 (2001) 535–544.
[15] C.T. Hseih, W.L. Huang, J.T. Lue, The change from paramagnetic resonance to ferromagnetic resonance for iron nanoparticles made by the sol–gel method, J. Phys. Chem. Sol. 63 (2002) 733–741.
[16] J.L. Gould, J.L. Kirschvink, K.S. Deffeyes, Bees have magnetic remanence, Science 201 (1978) 1026–1028.
[17] B.A. Maher, Magnetite biomineralization in termites, Proc. Roy. Soc. Lon. B 265 (1998) 733–737.
[18] E.M. Yahiaoui, R. Berger, Y. Servant, J. Kliava, L. Cugunov, A. Mednis, Electron-paramagnetic-resonance of Fe^{3+} ions in borate glass–computer-simulations, J. Phys. Condens. Matter 6 (1994) 9415–9428.
[19] E. Wajnberg, L.J. El-Jaick, M.P. Linhares, D.M.S. Esquivel, Ferromagnetic resonance of horse spleen ferritin: core blocking and surface ordering temperatures, J. Magn. Reson. 153 (2001) 69–74.
[20] J.K. Grady, Y. Chen, N.D. Chasteen, D.C. Harris, Hydroxyl radical production during oxidative deposition of iron in ferritin, J. Biol. Chem. 264 (1989) 20224–20229.
[21] H. Nichol, M. Locke, The localization of ferritin in insects, Tissue cell 22 (1990) 767–777.
[22] M. Kimura, L. Seveus, K. Maramorosch, Ferritin in insect vectors of maize streak disease agent—electron-microscopy and electron-microprobe analysis, J. Ultra. Mol. Struct. Res. 53 (1975) 366–373.
[23] S.A. Makhlouf, F.T. Parker, A.E. Berkowitz, Magnetic hysteresis anomalies in ferritin, Phys. Rev. B 55 (1997) R14717–14720.
[24] M.E.Y. Mohie-Eldin, R.B. Frankel, L. Gunther, A comparison of the magnetic-properties of polysaccharide iron complex (pic) and ferritin, J. Magn. Magn. Mater. 135 (1994) 65–81.
[25] C. Quintana, M. Lacin, C. Marhic, M. Perez, J. Avila, J.L. Carrascoa, Initial studies with high resolution TEM and electron energy loss spectroscopy studies of ferritin cores extracted from brains of patients with progressive supranuclear palsy and Alzheimer disease, Cell. Mol. Biol. 46 (2000) 807–820.
[26] P.M. Harrison, P. Arosio, Ferritins: molecular properties, iron storage function and cellular regulation, Biochim. Biophys. Acta 1275 (1996) 161–203.
[27] J. Dobson, Nanoscale biogenic iron oxides and neurodegenerative disease, FEBS Lett. 496 (2001) 1–5.
[28] K. Abe, Y. Miyamoto, S. Chikazumi, Magnetocrystalline anisotropy of low-temperature phase of magnetite, J. Phys. Soc. Jpn. 41 (1976) 1894–1902.
[29] Z. Kakol, J.M. Honig, Influence of devietions from ideal stoichiometry on anisotropy parameters of magnetite $Fe_{3(1-\delta)}O_4$, Phys. Rev. B 40 (1989) 9090–9097.
[30] K.P. Belov, Electronic processes in magnetite (magnetite mysteries), Phys. Uspekhi 36 (1993) 380–391.
[31] V.A.M. Brabers, F. Walz, H. Kronmuller, Impurity effects upon the Verwey transition in magnetite, Phys. Rev. B 58 (1998) 163–166.
[32] Y.A. Koksharov, D.A. Pankratov, S.P. Gubin, I.D. Kosobudsky, M. Beltran, Y. Khodorkovsky, A.M. Tishin, Electron paramagnetic resonance of ferrite nanoparticles, J. Appl. Phys. 89 (2001) 2293–2298.
[33] M. Hagiwara, K. Nagata, K. Nagata, Magnetism and magnetic interaction in a complex oxide glass system containing deposited clusters of magnetite at the superparamagnetic state, J. Phys. Soc. Jpn. 67 (1998) 3590–3600.
[34] P.A.A. van der Heijden, M.G. van Opstal, C.H.W. Swüste, P.H.J. Bloemen, J.M. Gaines, W.J.M. Jonge, A ferromagnetic resonance study on ultra-thin Fe_3O_4 layers grown on (0 0 1)MgO, J. Magn. Magn. Mater. 182 (1998) 71–80.
[35] J. Tang, K. Wang, W. Zhou, Magnetic properties of nanocrystalline Fe_3O_4 films, J. Appl. Phys. 89 (2001) 7690–7692.
[36] S. Kale, S.M. Bhagat, S.E. Lofland, T. Scabarozi, S.B. Ogale, A. Orozco, S.R. Rhinde, T. Venkatesan, B. Hannoyer, B. Mercey, W. Prellier, Film thickness and temperature dependence of the magnetic properties of pulsed-laser-deposited Fe_3O_4 films on different substrates, Phys. Rev. B 64 (2001) 205413.
[37] M.S. Seehra, A. Punnoose, A. Manivannan, Effect on Si doping on the electron spin resonance properties of ferrihydrite nanoparticles, IEEE Trans. Magn. 37 (2001) 2207–2209.
[38] M. Rickli, R.H. Leuthold, Homing in harvester termites—evidence of magnetic orientation, Ethology 77 (1988) 209–216.
[39] D. Schuler, Molecular analysis of a subcellular compartment: the magnetosoma membrane in *Magnetospirillum gryphiswaldense*, Arch. Microbiol. 181 (2004) 1–7.
[40] D.M.S. Esquivel, H.G.P. Linsde Barros, M. Farina, Diversity of magnetic crystals found in magnetotactic bacteria, in: R.B. Frankel, R.P. Blakemore (Eds.), Iron Biominerals, Plenum Press, New York, 1991.
[41] E. Wajnberg, G.R. Cernicchiaro, D.M.S. Esquivel, Antennae: the strongest magnetic part of the migratory ant, Biometals (2004) in press.
[42] D.M.S. Esquivel, E. Wajnberg, G.R. Cernicchiaro, O.C. Alves, Comparative magnetic measurements of migratory ant and its only prey, J. Mag. Mat. (2004) in press.